Microscopic ESPI:
Better fringe quality by the Fourier transform method

Akram El Jarad, Gerd Gülker, Klaus D. Hinsch
Carl von Ossietzky University Oldenburg, Department of Physics, P.O.: 2503
26111 Oldenburg, Germany

ABSTRACT

Electronic speckle pattern interferometry (ESPI) is discussed for the detection of out-of-plane deformations in small objects. For increasing the resolution in object space a laser source of small wavelength is combined with a microscope with a high numerical aperture. Fringe quality is increased by using spatial phase-shifting and the Fourier transform method to allow deformation detection also under non-optimum conditions. The efficacy will be shown in some measurements on different specimens where deformations are successfully recorded in areas down to a few micrometers in size.

Keyword : microscope, ESPI, Fourier transform method, spatial phase shift

1. INTRODUCTION

Electronic speckle pattern interferometry (ESPI) is normally used for detecting deformations in objects of a few centimetres to some metres in size. Meanwhile, the growing need to investigate the behaviour of micro-components[1,2] requires measurements on much smaller objects. Microscopic ESPI is also used in medical measurements[3]. In the literature one finds even more experimental work using microscopic ESPI[4,5,6].

For similar purposes we have realized an ESPI set-up using a microscope for observation. As a result of the high numerical aperture the speckle size in object space is very small. In chapter 2.1 we will discuss the basic speckle size problem in microscopic ESPI. By using the classical subtraction method even smallest displacements of the specimen result in rapid decorrelation caused by the small speckle size in object space. In chapter 2.2 we will demonstrate how the use of spatial phase shifting[7] and the Fourier transform method can compensate some of these decorrelations.

We will present an experimental set-up for microscopic ESPI in chapter 3. The best way is discussed to introduce the reference beam for optimum spatial phase-shift. A measurement on a tilted plate (chapter 4.1) will demonstrate the efficacy of using the Fourier transform method. Some typical measurements are shown on specimens, where deformations are found within regions of as little as a few micrometers.

2. THEORY

2.1 Microscopic ESPI

Lokberg et al.[8] have described in detail the basic theory of microscopic ESPI and the resulting problems. Thus, it suffices to refresh only the important results. We will show the differences to normal ESPI and give a solution for a great problem in the microscopic case.

Fig. 1 shows a typical kind of microscope with a tube lens for imaging. The magnification is given by the quotient of the focal lengths of tube lens f_{tube} and microscope objective f_{MO}:

$$M = \frac{\overline{A'B'}}{\overline{AB}} = \frac{f_{tube}}{f_{MO}} \tag{1}$$

By illuminating a rough-surface object with coherent light, there will arise speckle patterns in the image plane. The speckle size d_S is given by[9]

$$d_S = 1.22\lambda F_{eff} = 1.22\lambda \frac{D}{f_{tube}}, \tag{2}$$

where λ is the wavelength used and F_{eff} the effective exit aperture, in this case the quotient of diameter of the limiting aperture D and the imaging distance f_{tube}. With the Abbe sine condition, we get

$$d_S \approx 1.22\lambda \frac{M}{2NA}, \tag{3}$$

where NA is the numerical aperture of the objective.
The resolution in object space is limited by the speckle diameter d_S backprojected onto the object

$$d_A = d_S / M \approx 1.22\lambda \frac{1}{2NA}. \tag{4}$$

Normally it is assumed that an area of 5 x 5 speckles is needed to detect a deformation. By increasing the numerical aperture NA and reducing the wavelength λ we increase the resolution in object space and thus reduce the minimum possible area on which a deformation can be detected.
In the same way the speckle length

$$l_S \approx 2\lambda \frac{M}{NA^2} \tag{5}$$

can be backprojected on the object:

$$l_{S,O} = l_S / M \approx 2\lambda \frac{1}{NA^2}. \tag{6}$$

However, displacements of the specimen result in a shift of the specklefield.
In the classical subtraction method for ESPI the interferograms or phasemaps will be directly subtracted. Thus specimen displacements result in decorrelations. If the shift of the speckle field is about one speckle size or length, the subtracted image is totally decorrelated. Because of $d_A > l_{S,O}$ the main decorrelation is given by the in-plane displacement. In normal ESPI, where the speckle size in object space is large, small displacements of the specimen have only a small change of the speckle field as result. But using high magnifications result in a large shift of the speckle field in image

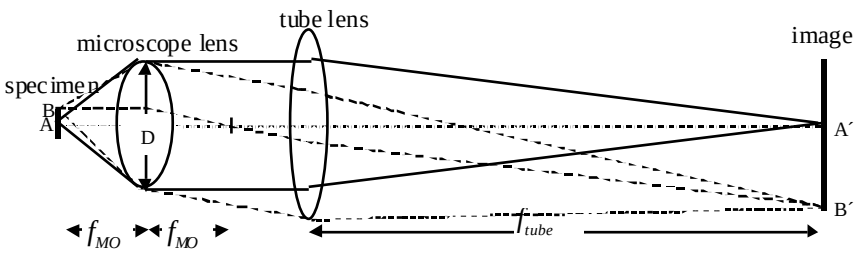

Fig. 1: Principal lay-out of tube lens microscope

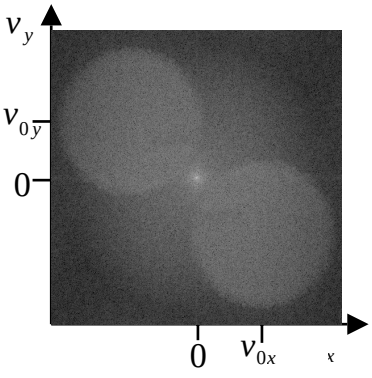

Fig. 2: Power spectrum of a spatially phase biased interferogram

space. Therefore it is useful to shift back the interferogram, to reduce the decorrelation effects of in-plane displacements by the specimen. Thus we have no more limitation of the magnification, which is given by in-plane displacements, which are small to the field of view. By using the Fourier transform method we can calculate the shift of speckle field. Microscopic ESPI without back-shifting is only possible under optimum conditions of stability and as result only in particularly cases.

2.2 Spatial phase shifting and Fourier transform method

Spatial phase shifting is a good method to minimize phase variation from interferometric measurements. The needed phase shifted data are obtained at the same time but in different spaces of the image. In our case, we have realized the phase shift by shifting the origin of the reference beam from the centre of the aperture, as shown in Fig. 4. As superposition of reference and object beam we get a linear phase bias over the image. The disadvantage of spatial phase shifting is the use of bigger speckle size in image space to satisfy the Nyquist theorem. For using spatial phase shifting the speckle size should be between 2 d_p and 3 d_p, where d_p is the pixel pitch of the CCD-target, while in temporal phase shifting 1 d_p is sufficient. To produce bigger speckle sizes the limiting aperture has to be reduced. This causes a loss of resolution and light. In microscopic ESPI illumination is mostly no problem because of the small object sizes. A laser with only a few mW output power is sufficient. Also speckle sizes in microscopic ESPI are normally anyway bigger than necessary. Therefore there is no reason in microscopic ESPI against spatial phase shifting.

The intensity $I(x, y)$ of an interferogram with a linear phase-bias between object and reference wave, which have the same state of polarisation and same beam intensity, is given by

$$I(x, y) = |O(x, y) + R(x, y) \exp(-2\pi i (\nu_{0x} x + \nu_{0y} y))|^2, \tag{7}$$

where $O(x, y)$ and $R(x, y)$ are the complex amplitudes of object and reference waves and ν_{0x} and ν_{0y} are the spatial carrier frequencies. For a smooth reference wave with no phase variations, we can assume $R(x, y) = R_0$. For ESPI the object wave $O(x, y)$ is a speckle field. The spectrum $\tilde{I}(\nu_x, \nu_y)$ is given by the Fourier transform of Equation (7)

$$\tilde{I}(\nu_x, \nu_y) = \mathrm{FT}(|O|^2) + |R_0|^2 \delta(\nu_x, \nu_y) + R_0 \tilde{O}^*(-\nu_x - \nu_{0x}, -\nu_y - \nu_{0x}) + R_0^* \tilde{O}(\nu_x - \nu_{0x}, \nu_y - \nu_{0x}) \tag{8}$$

with $\tilde{O} = \mathrm{FT}(O)$ the Fourier transform of the object wave amplitude and * denotes the conjugate complex. This spectrum is a superposition of the speckle halo, the central peak und the two sidebands, in Equation (8) from left to right. In Fig. 2 an example of a spatially smoothed power spectrum $|\tilde{I}|^2$ is shown in logarithmic scale. The frequencies ν_{0x} and ν_{0y} are given by the position of the centre of the sidebands. The sideband diameter is inversely proportional to the speckle diameter. Here the speckle diameter is about 2.5 d_p.

We select one sideband by a suitable filter, shift it back by $(-\nu_{0x}, -\nu_{0y})$ to the origin of the frequency plane perform an inverse Fourier transform is given by

$$\mathrm{FT}^{-1}(R_0^* \tilde{O}(\nu_x, \nu_y)) = R_0^* O(x, y) = R_0^* |O(x, y)| \exp(i\varphi(x, y)) \tag{9}$$

where φ is the phase of the object wave. Normally, this is used to calculate the phase φ

$$\varphi(x, y) = \arctan\left(\frac{\mathrm{Im}[\mathrm{FT}^{-1}(R_0^* O(\nu_x, \nu_y))]}{\mathrm{Re}[\mathrm{FT}^{-1}(R_0^* O(\nu_x, \nu_y))]} \right), \tag{10}$$

but if we take the modulus squared of Equation (9) we get, except for a constant value, the intensity I_S of the object speckle field:

$$I_S(x, y) = |O(x, y)|^2. \tag{11}$$

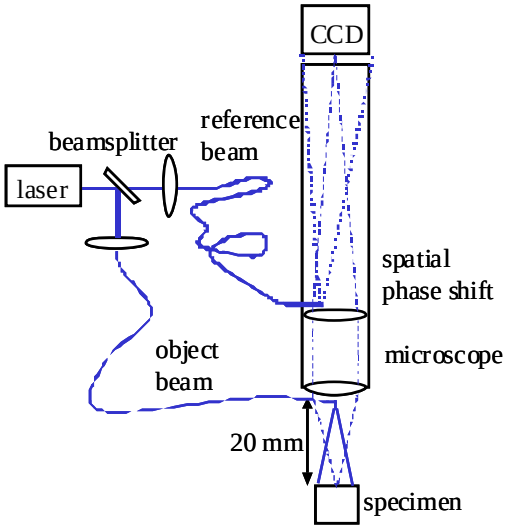

Fig. 4: Experimental set-up for microscopic ESPI

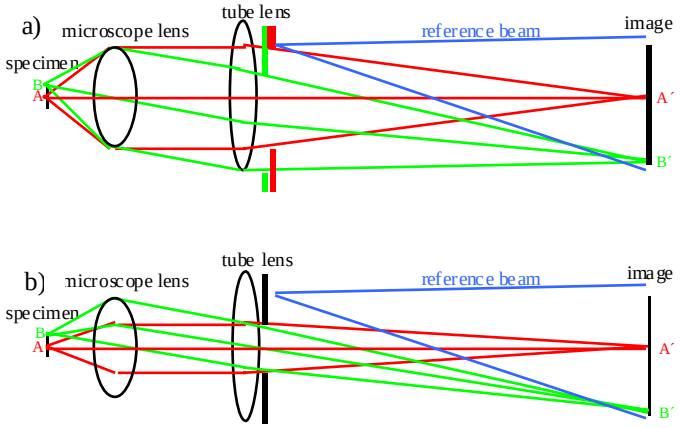

Fig. 3: Superposition of reference and object wave fronts, reference beam output at the exit of the tube lens a) if the microscope lens is limiting the aperture, virtual apertures are seen in green and red colour b) if the exit of the tube lens is set a limiting aperture (black)

By digital cross-correlation of the two speckle intensities before and after deformation, we can calculate the shift of the image with subpixel accuracy[10] from the position of the correlation peak. Shifting back the second interferogram by the calculated shift we get, except for a constant phase shift, nearly the same interferogram without the displacement of the specimen. By using this method we have no longer a limitation for small in-plane displacements of the specimen. Also the shift can be made for subimages. If there is an in-plane deformation each subregion can be shifted back for better fringe quality. Fricke-Begemann and Burke[11] have discribed in detail the method of shifting back the displacement, while normally it is used for better fringe quality, here it extends the use of microscopic ESPI.

3. SET-UP

The set-up used is shown in Fig. 4. Because of its small wavelength we use a Nd:YAG-Laser at 532 nm. The light to illuminate the specimen is guided by an optical fibre. For a high resolution in object space we use a microscope objective to image the specimen onto the camera. We have chosen the Mitutoyo infinity corrected objective M Plan APO 20 because of its long working distance of 20 mm. This makes it easy to illuminate the specimen. With its numerical aperture of 0.42, we obtain a speckle diameter in object space d_A of about 0.8 µm. To create the image on the CCD-target we use different simple tube lenses with focal lengths varying between 250 mm and 400 mm. With these lenses we get speckle diameters in image space between 2 d_p and 3 d_p. The CCD-camera used is an Adimec MX 12P with 8 bit dynamic resolution and 1024 x 1024 pixels. The effective pixel size is about 10 µm. The CCD-camera is placed in the focus of the tube lens. The given fields of view vary between 250 µm and 400 µm. The reference beam is also guided by a fibre. The fibre exit is held in a cannula. To obtain a linear phase-bias between object and reference wave over the CCD target it is necessary to place the fibre exit off-axis in the plane of the limiting aperture, which is in most microscopes the entrance of the microscope lens. By passing the microscope and the tube lens the reference beam suffers in quality because of reflections on the surfaces of the lenses. In addition, by passing two lenses it is very difficult to adjust the reference beam output position to have the wanted phase-bias over the image. We have chosen the position of the reference beam at the exit of the tube lens, because then the light does not have to pass any interfaces. Here the reference beam quality is very good. But the linearity of the phase-bias is not as good as when placing the reference output in the plane of the limiting aperture. In Fig 3 a it can be seen easily, that the virtual limiting aperture at the exit of the tube lens is different for the points A´ and B´. Thus the distances of the reference beam output from the centre of the virtual limiting apertures are different and therefore also the phase bias in the regions around these points. Therefore the phase bias over the image is not linear. By limiting the beam at the exit of the tube lens sufficiently by a limiting aperture, however, we obtain a linear phase bias even in case of Fig. 3 b. Then the limiting aperture is changed and in consequence the aperture of the microscope lens and therefore also the resolution will be reduced. For this reason we do not use a limiting aperture at the tube lens exit. Instead, we minimize the distance between the tube lens and the microscopic lens. Thus we get only a small difference in phase-bias.

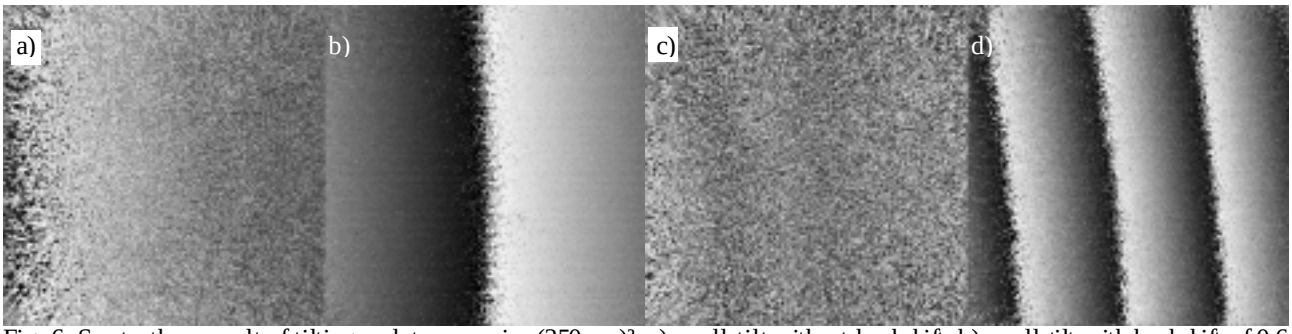

Fig. 6: Sawtooth as result of tilting a plate, area size (350 µm)², a) small tilt without backshift, b) small tilt with backshift of 0.6 speckle diameter, c) big tilt without backshift, d) big tilt with backshift of 1.2 speckle diameter

4. EXPERIMENTAL RESULTS

4.1 Tilted plate

A white metal plate is tilted for an out-of-plane deformation. If the tilting axis, however, is not exactly in the plate surface nor in the middle of the observed area the tilt produces an additional in-plane displacement. In chapter 2.1 we have shown that a microscopic ESPI is especially sensitive to in-plane displacement of the specimen. As result of a tilt we get a high decorrelation with the classical subtraction method. Shifting back the image before calculation and subtraction of phasmaps results in better fringe quality. Such results are shown in Fig. 6. Fig. 6 a shows the improvement without back-shifting. It is possible to detect a tilt, but it is very noisy. Fig. 6 b shows the subtracted phasemap with a backshift of about 0.6 speckle diameter. In Fig. 6 c and d the tilt and therefore the displacement are bigger. There is no more information about the tilt without back-shifting the interferogram. The fringe quality of backshifted sawtooth image is even very good. This examples show that the fringe quality is much better using the Fourier transform method for shifting back the images. We can detect a deformation although there is a considerable in-plane displacement.

4.2 Small area sized deformation of a gold-leaf

In Fig. 5 the following specimen is shown. A gold-leaf is put onto an alginat ceramic, which is a special directed-structure material. It is provided with parallel capillaries of about 11 µm in diameter. The capillaries are arranged vertical to the measured surface.

We can deform the gold-leaf by applying a negative pressure to the backside of the ceramic. The thin gold-leaf is then sucked partly into the capillaries.

Fig. 7 a shows the white-light microscopic image of the ceramic with the measured of 350 µm in size. One resulting deformation from an ESPI measurement is shown in Fig. 7 b. The obtained deformations, seen in the sawtooth image, are found in

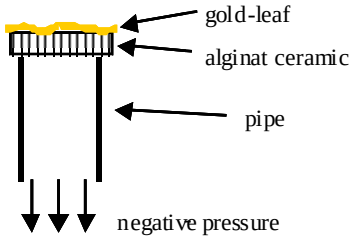

Fig. 5: Specimen for test measurement: a gold-leaf is put on a directed-structure ceramic

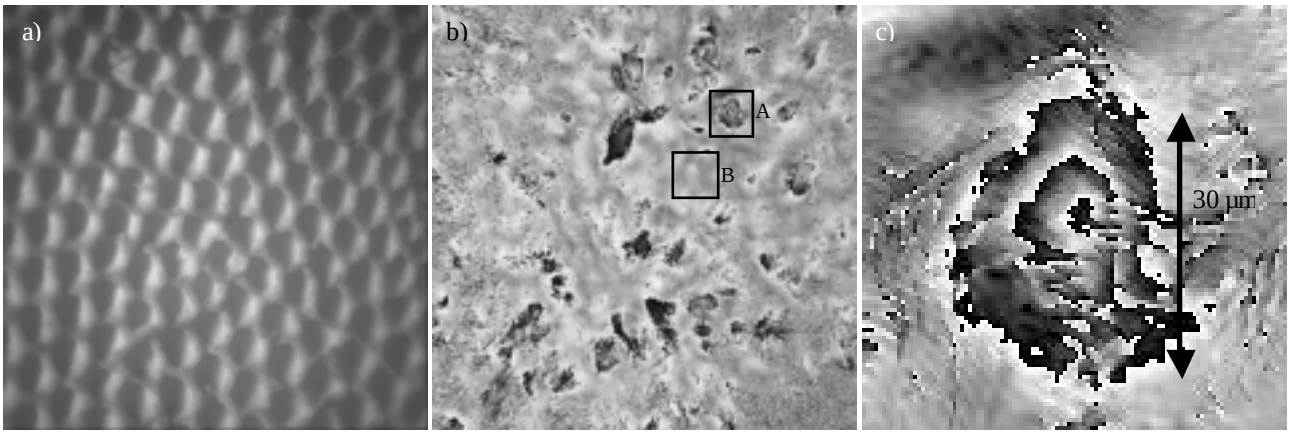

Fig. 7 a) white-light microscopic photo of the directed-structure ceramic, area size (350 µm)² b) sawtooth image of out-of plane deformation of the gold-leaf by producing a negative pressure, same area, c) elevation of the subregion A indicated in b)

regions sized slightly more than a capillary. The amplitude varies. Some capillaries show big deformations of a few micrometers (for example in region A), others only some ten nanometers (for example in region B). It can be explained by different starting situations and with inhomogeneity of the capillaries, thus the used negative pressure to deform the gold-leaf is different. In areas with big deformation we can detect a change of grey value with resolution down to a few pixels or a few micrometers in object space, as is seen in the elevation of the region A in Fig. 7 c. In this small region of about 30 µm it can be detected more than one sawtooth. The correlation is very high because the gold-leaf is a reflecting surface, and as result there are regions without speckle patterns. Thus the quality of the sawtooth is very good.

4.3 Measurement on an ancient coloured fragments while humidity change

An example for deformations on microscopic scale which is found in nature are coloured fragments where the paints sometimes have microscopic cracks which have as result small sub-regions, which deform itself while a change of humidity. We have investigated deformations on coloured fragments of the famous 2000-yr-old terracotta army of the first Chenise emperor[4]. For changing the climate conditions we have constructed a special climate chamber, where we let pass conditioned air. This cause unwanted effects of vibrations and small displacements of specimen. The region of detection has an edge length of 230 µm. While drying the painting deform in the sub-areas, to a form like a bowl. An example of sawtooth image is shown in Fig. 8. The images are shifted back by Fourier transform method. Beside, for this measurement it is very important to use spatial phase shifting for getting the interferogram from a single image to reduce the imaging time interval. By following the sawtoothes we can detect cracks. Most sub-areas have a size of about 50 µm in diameter with a maximum deformation of about 500 nm. At the left part of the image there are bigger sub-areas, which deform much more. At the left bottom of the image the deformation is very large in with consequence of a high in plane displacement. In Fig. 8 a the whole image is shifted back. In the Fig. 8 b right image the shifts are made in subimages of 128 pixel in size. Then the correlation is much higher. We can also detect deformations in the left bottom region.

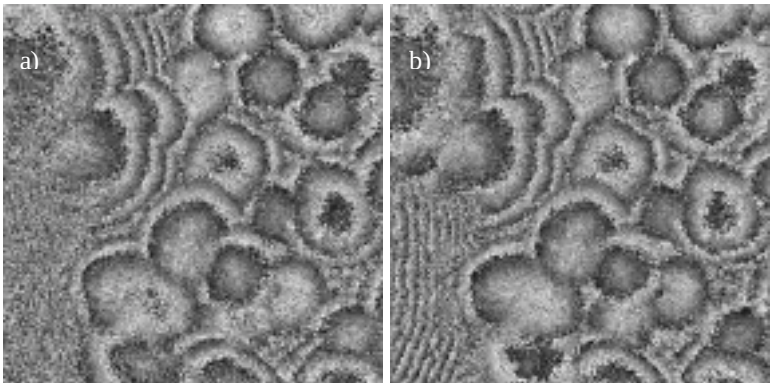

Fig. 8: Investigation of coloured terracotta fragment with an area size of 230 x 230 µm². a) backshift of total image, b) backshift of subimages with 128 Pixel x 128 Pixel in size.

5. CONCLUSIONS

In this paper we have shown who to extend microscopic ESPI measurement by using the Fourier transform method. The influence of in-plane displacements of the specimen can be reduced by shifting back the intefreogram with subpixel precision. Together with spatial phase shifting it is possible to use microscopic ESPI also under non-optimum conditions of stability. We have shown with some example measurements the efficacy of this method.

ACKNOWLEGEMENT

The authors thank the DFG for finacial support. For getting the directed-structure ceramic we thank the "Labor für Grenzflächenchemie" of the University of Regensburg.

REFERENCES

1. H. A. Aebischer and E. Mazza, "Measurement of the nanometre deformation field in metallic microbars with microscopic ESPI", Proc. Spie, 3098, pp. 400-410, 1997.
2. P. Aswendt and R. Hofling, "Testing microcomponents by speckle interferometry", Opt. Las. Eng., 26, pp. 313-330, 1997.
3. P. Neiswander and G. A. Slettemoen, "Electronoc speckle pattern interferometric measurements of the basilar membrane in inner ear", Appl. Opt., 20.24, pp. 4271-4276, 1981.
4. G. Gülker, K. D. Hinsch and A. Kraft, "Deformation monitoring on ancient terracotta warriers by microscopic TV-holography", Opt. Las. Eng., 36, pp. 501-513, 2001.

5. M Aslan and B. R. Tittmann, “Laser interferometry for measurements of displacements“, Proc. Spie., 3993, pp. 68-77, 2000.
6. D. P. Herbert, “Inspection of out-of-plane surface movements over small areas using electronic speckle pattern interferometry“, Opt. Las. Eng., 4, pp. 229-239, 1983.
7. T. Bothe, J. Burke and H. Helmers,”Spatial phase shifting in ESPI: minimization of phase reconstruction errors”, Appl. Opt., 36.22, pp. 5310-5316, 1997.
8. O. J. Lokberg, B. E. Seeberg and K. Vestli, “Microscopic video speckle interferometry“, Opt. Las. Eng., 26, pp. 313-330, 1997.
9. J. W. Goodman, “Statistical Properties of Laser Speckle Patterns”, Laser and Speckle and Related Phenomena, J. C. Dainty, Springer Verlag, Berlin, 1975.
10. M. Sjödahl and L. R. Benchert, “Electronic speckle photography: analysis of an algorithm giving the displacement with subpixel accuracy”, Appl. Opt., 32.13, pp. 2278-2284, 1993.
11. T. Fricke-Begemann, and J. Burke, “Speckle interferometry: Three-dimensional deformation field measurement using a single interferogram”, Appl. Opt., 40.28, pp. 5011-5022, 2001.